Quantitative DCE-MRI Evaluation of Breast Cancer Response to Neoadjuvant Chemotherapy

Alina Tudorica[1], Karen Y Oh[1], Stephen Y-C Chui[1], Nicole Roy[1], Megan L Troxell[1], Arpana Naik[1], Kathleen A Kemmer[1], Yiyi Chen[1], Megan L Holtorf[1], Aneela Afzal[1], Charles S Springer[1], Xin Li[1], and Wei Huang[1]

[1]*Oregon Health & Science University, Portland, OR, United States*

Introduction: Neoadjuvant chemotherapy (NACT) is increasingly used to treat locally advanced breast cancer, allowing breast conservation surgery for patients with reduced disease burden following treatment. In addition, pathologic complete response (pCR) to NACT is prognostic for survival (1). However, most patients do not achieve pCR and, in any case pathologic response can be determined only after surgery. Thus, there is an urgent need for minimally invasive methods to provide early prediction of therapy response, potentially allowing rapid, personalized treatment plan alteration for non-responding patients. By measuring tumor microvascular properties, quantitative dynamic contrast-enhanced (DCE) MRI has been shown capable of providing early prediction of breast cancer response following 1-2 NACT cycles (2-4). Most published studies employed the Standard (Tofts) model (SM) for pharmacokinetic analysis of DCE-MRI data, and few reported relationships between DCE-MRI parameters and residual disease burden. Here we report our preliminary results in DCE-MRI assessment of breast cancer response to NACT when DCE-MRI data were analyzed using both the SM and the Shutter-Speed model (SSM). The SSM accounts for finite transcytolemmal water exchange kinetics (5). DCE-MRI metrics including the SSM-unique τ_i parameter (mean intracellular water lifetime), an inverse measure of cellular energy metabolism (6,7), were evaluated and compared with imaging tumor size measurement for early prediction of response and assessment of residual disease.

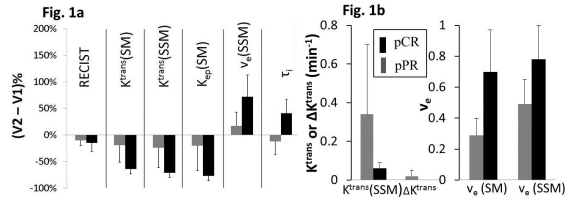

Methods: 21 consecutive patients with locally advanced breast cancer and to begin NACT consented to research DCE-MRI studies performed at Visit 1 (V_1) - before NACT, V_2 - after first NACT cycle, V_3 – midpoint of NACT (usually after three NACT cycles), and V_4 - after NACT completion. Axial bilateral DCE-MRI images with fat-saturation and full breast coverage were acquired with a 3D gradient echo-based TWIST sequence (8) using a 3T Siemens scanner. DCE-MRI acquisition parameters included 10° flip angle, 2.9/6.2 ms TE/TR, a parallel imaging acceleration factor of two, 30-34 cm FOV, 320x320 matrix size, and 1.4 mm slice thickness. The total acquisition time was ~ 10 min for 32-34 image volume sets with 14-20 s temporal resolution. Gd contrast agent (Prohance®) IV injection (0.1 mmol/kg at 2 mL/s) was timed to start following acquisition of two baseline image volumes. Tumor ROIs were drawn on post-contrast DCE images by experienced radiologists who also measured tumor size according to the (one dimensional) RECIST (9) guidelines. The ROI-averaged and pixel-by-pixel (within the ROI) DCE time-course data were subjected to both the SM and SSM pharmacokinetic analyses to extract K^{trans}, v_e, k_{ep} (= K^{trans}/v_e), and τ_i (SSM only) parameters. The ΔK^{trans} parameter [= K^{trans}(SSM) - K^{trans}(SM)], a measure of water exchange effects on K^{trans} estimation (5), was also calculated. The whole tumor mean parameter value was calculated as the weighted (by ROI pixel number) average of the single-slice ROI values from the image slices covering the entire tumor.

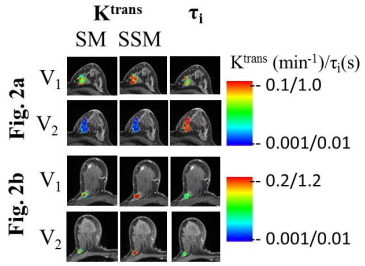

The pathologic response to NACT and residual cancer burden (RCB) for each patient were determined by pathology analysis of post-NACT resection specimens and comparison with pre-NACT core biopsy specimens using previously published methods (10). The pathology endpoints were correlated with the MRI metrics using the univariate logistic regression (ULR) analysis and the Spearman's correlation (SC) to identify imaging biomarkers for early prediction of response and/or accurate assessment of RCB following NACT.

Results: Pathology analyses revealed that 5 patients achieved pCR – no invasive cancer cell found in resection specimens, while the other 16 were pathologic partial responders (pPR) – reduced cancer cell density in resection specimens compared to biopsy specimens. The ULR analysis found that the % changes in tumor mean k_{ep}(SM), τ_i, v_e(SSM), and K^{trans}(SM and SSM) after the first NACT cycle (at V_2 relative to V_1) were excellent early discriminators of the pCRs from the pPRs, or non-pCRs, with ULR c statistics values = 0.975, 0.938, 0.906, 0.900, and 0.900 (c is equivalent to area-under-the-curve of ROC analysis), respectively; while the early RECIST % change was a poor predictor of response with c = 0.619. **Fig. 1a** shows a mean±SD column graph of the % changes of these MRI metrics for the pCR (black) and pPR (gray) groups. Except for RECIST, the difference between the two groups was statistically significant ($P < 0.05$) in all plotted DCE-MRI metrics. Additionally, the absolute values of V_2 mean ΔK^{trans} and histogram median values of K^{trans}(SSM) and v_e (SM and SSM) (**Fig. 1b**) were also good to excellent (c = 0.969, 0.906, 0.875, and 0.844, respectively) early predictors of response. The ΔK^{trans} column for the pCR group is almost invisible in Fig. 1b because its mean value was near zero. **Fig. 2** shows tumor K^{trans}(SM), K^{trans}(SSM), and τ_i color maps of a pCR (2a) and a non-pCR (2b) at V_1 and V_2, demonstrating substantial K^{trans} decreases and τ_i increase for the pCR, but minimal changes for the non-pCR. The RCB can be described in numerical values or stratified in ranks (such as I, II, III, *etc.*) with RCB = 0 for pCR (10). ULR and SC analyses were used to correlate V_4 MRI metrics with RCB rank and actual value, respectively. The **Table** shows that V_4 tumor mean τ_i and K^{trans}(SM and SSM) were good (c = 0.8 - 0.9), while V_4 RECIST was a fair (c = 0.7 – 0.8), measure of RCB rank. The SC analysis (**Fig. 3**) reveals that V_4 K^{trans} and RECIST were positively, while τ_i was inversely, correlated with RCB value. These correlations were statistically significant ($P < 0.01$).

Table. Predicting the RCB Rank	
V_4 MRI Metrics	**ULR c Value**
V_4 mean τ_i	0.832
V_4 mean K^{trans}(SSM)	0.815
V_4 mean K^{trans}(SM)	0.811
V_4 RECIST	0.780

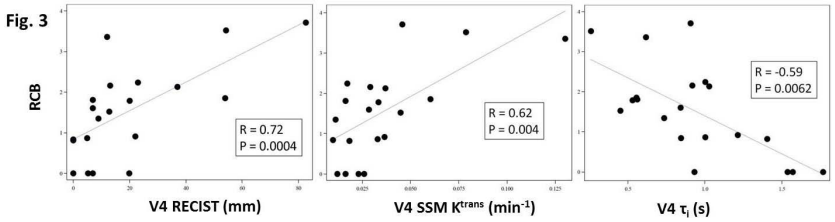

Discussion and Conclusion: Consistent with previous studies (2-4), our preliminary results indicate that changes in breast tumor microvasculature as measured by DCE-MRI are much better early predictors of NACT response than tumor size change. After only one NACT cycle, the % changes or absolute values of several quantitative DCE-MRI biomarkers can provide excellent predictions of eventual pathologic response, potentially playing an important role in personalized care of breast cancer patients in the future. Evaluation of tumor size is the current standard-of-care in assessing therapy response. Our results show that RECIST measure of tumor size is a poor early predictor of response, though it is a valuable marker of RCB after NACT completion. The K^{trans} parameter derived from either the SM or the SSM analysis is an excellent early predictor of response and a good marker of RCB. However, the use of the SSM for DCE-MRI data analysis also allows access to the τ_i biomarker and adds a metabolic dimension (6,7) in evaluation of therapy response. The utility of the τ_i parameter is clearly demonstrated in early prediction of response and accurate assessment of residual disease, with τ_i increase often coinciding with K^{trans} and/or k_{ep} decrease. The ability of the SSM DCE-MRI method to characterize synergistic microvascular perfusion and cellular energetic metabolism simultaneously may harbor great promise for studying tumor microenvironment, and its response to therapy.

Grant Support: NIH UO1-CA154602.

References: **1.** Kong *et al. Eur J Cancer* 2011;47:2084-90. **2.** Marinovich *et al. The Breast* 2012;21:669-677. **3.** Li *et al. Trans Oncol* 2014;7:14-22. **4.** Ah-See *et al. Clin Cancer Res* 2008;14:6580-9. **5.** Huang *et al. Radiology* 2011;261:394-403. **6.** Zhang *et al. Biophys J* 2011;101:2833-42. **7.** Springer *at al. NMR Biomed* 2014;27:760-73. **8.** Tudorica *et al. Magn Reson Imaging* 2012;30:1257-67. **9.** Therasse *et al. J Natl Cancer Inst* 2000;92:205-16. **10.** Symmans *et al. J Clin Oncol* 2007;25:4414-22.